

# Observations of nonlinear elastic wave behavior in sandstone

G. Douglas Meegan, Jr., Paul A. Johnson, Robert A. Guyer,<sup>a)</sup> and Katherine R. McCall  
*Earth and Environmental Sciences Division, Mail Stop D443, Los Alamos National Laboratory,  
Los Alamos, New Mexico 87545*

(Received 17 August 1992; accepted for publication 12 August 1993)

An experimental investigation of nonlinear elastic wave behavior was conducted using a 2-m-long cylindrical rod of Berea sandstone in order to study the strong elastic nonlinearity that is characteristic of microcracked materials. Measurements of the displacement field at distance  $x$  from the source show rich harmonic content with harmonic amplitudes depending on  $x$ , source frequency, and source amplitude. The amplitude of the  $2\omega$  harmonic is found to grow linearly with  $x$  and as the square of both the source frequency  $\omega$  and the source amplitude  $U$ . This behavior is in agreement with the predictions of nonlinear elasticity theory for a system with cubic anharmonicity. From the measured amplitude of the  $2\omega$  harmonic the parameter  $|\beta|$ , a measure of the strength of the cubic anharmonicity, is found to be of order  $10^4$  ( $7.0 \times 10^3 \pm 25\%$ ). This value is orders of magnitude greater than that found in ordinary uncracked materials. These results suggest that wave distortion effects due to nonlinear elasticity can be large in seismic wave propagation and significantly influence the relationship of seismic signal to seismic source.

PACS numbers: 43.25.Dc

## INTRODUCTION

Since the late 1950s there has been a great deal of research in nonlinear acoustic wave propagation. In particular, observations of nonlinearly produced harmonic growth in gases,<sup>1</sup> liquids,<sup>2,3</sup> and uncracked solids have been made.<sup>4</sup> Such experiments show that nonlinear effects can take place along the wave propagation path well away from an acoustic or elastic wave source. More recently, there has been increasing interest in nonlinear wave processes in cracked solids and porous media which are characterized by strong elastic nonlinearity.<sup>5,6</sup> Earth materials are an important example of this type of disordered media because of their practical importance in geophysics and seismology. Only recently, laboratory and field experiments have demonstrated that significant nonlinear wave effects do indeed exist in earth materials.<sup>7-12</sup> In this paper, we present the results of a laboratory study of harmonic growth in compressional waves as a function of amplitude, frequency, and propagation distance in Berea sandstone.

In Sec. I, we review the results of the theoretical description of acoustic wave propagation in a nonlinear material having cubic anharmonicity. We draw attention to the dependence of the amplitude of the  $2\omega$  harmonic on source frequency, source amplitude, and the separation between source and detector. In Sec. II, we describe the experimental system. We present and describe the experimental results in Sec. III. We show qualitative evidence for the presence of nonlinearity in the response of the elastic system. Further, we show quantitative evidence that part of this response is due to enormous cubic anharmonicity in

the elasticity of the system. We determine the strength of the cubic anharmonic parameter  $\beta$ . We summarize our findings in Sec. IV.

## I. THEORETICAL BACKGROUND

The equation of motion for a homogeneous elastic solid, to second order in the displacement (cubic anharmonicity in the elastic moduli), is derived in several texts.<sup>13-15</sup> The inclusion of linear attenuation modifies the equation.<sup>16-18</sup> Here we quote the results for elastic wave propagation in the absence of attenuation. Later, in our analysis, we assess the importance of attenuation. For a longitudinal plane wave propagating in the  $x$  direction, the equation of motion in the absence of attenuation is<sup>18</sup>

$$\frac{\partial^2 u(x,t)}{\partial x^2} - \frac{1}{c^2} \frac{\partial^2 u(x,t)}{\partial t^2} = -\beta \frac{\partial}{\partial x} \left( \frac{\partial u(x,t)}{\partial x} \right)^2, \quad (1)$$

where  $\beta$  is the nonlinear coefficient defined as

$$\beta = \frac{3(\lambda + 2\mu) + 2(l + 2m)}{2(\lambda + 2\mu)},$$

$u(x,t)$  is the particle displacement,  $c$  is the compressional velocity,  $\lambda$  and  $\mu$  are second-order elastic moduli (Lamé coefficients), and  $l$  and  $m$  are third-order elastic moduli (Murnaghan coefficients).

The interaction of the displacement with itself (the nonlinear interaction), the term on the right-hand side of Eq. (1), causes the creation of sum and difference frequencies and the breakdown of the wave superposition principle. Equation (1) can be solved analytically by an iterative

<sup>a)</sup>Permanent address: Department of Physics, University of Massachusetts, Amherst, MA 01003.

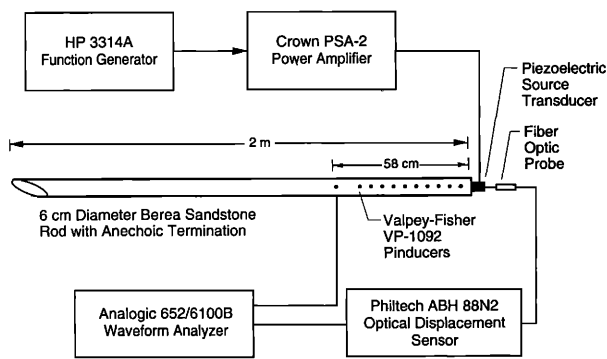


FIG. 1. Experimental setup.

Green's function technique. Solution to this equation for a source at the origin of frequency  $\omega$  and amplitude  $U$  is, to first order in the nonlinearity,

$$u(x,t) = u_0(x,t) + u_1(x,t) \\ = Ue^{i(kx - \omega t)} + (\beta U^2 k^2 x/2)e^{i(2kx - 2\omega t)}, \quad (2)$$

where  $u_0(x,t)$  is the displacement solution to the linearized equation of motion, and  $u_1(x,t)$  is the first-order correction to  $u_0(x,t)$  due to the nonlinear interaction. In principle, Eq. (1) can be solved to higher order,<sup>18</sup> i.e.  $u = u_0 + u_1 + u_2 + u_3 + \dots$ , but here we will only consider the first-order nonlinear term. This method of solution is valid as long as the energy transferred from frequency  $\omega$  to its harmonics is a small fraction of the total energy.

Note that a source at the origin of frequency  $\omega$  and initial displacement amplitude  $U$  generates a plane wave at frequency  $\omega$  with amplitude  $U$  and a second plane wave at frequency  $2\omega$  whose amplitude grows linearly with the distance of propagation  $x$ , the square of the fundamental frequency  $\omega$ , and the square of the fundamental amplitude  $U$ . In our experiment, we test the distance, frequency, and amplitude dependence of the  $2\omega$  harmonic in relation to the fundamental.

## II. APPARATUS AND MEASUREMENT METHODS

The apparatus used in the experiments is shown in Fig. 1. A 2-m-long, 6-cm-diam cylindrical sample of Berea sandstone was machined for the experiment. One end of the rod was tapered in order to minimize reflections. To accommodate the receiving transducers, eleven 0.3-cm-diam holes were drilled in the rod at intervals of 5 cm along a distance of 58 cm from the source transducer. The holes were drilled into the center of the rod at a 45 deg angle. Valpey-Fisher VP-1092 pin-shaped transducers (pinducers) were used as detectors. The pinducers are standard piezoelectric material set inside the bottom end of a thin hollow tube. (The detector sensitivity is at a maximum for waves propagating parallel to the long axis of the pinducers. This geometry was impossible to obtain. Therefore, the pinducers were placed at 45 deg from the axis where their response was still very good.)

A self-monitoring drive transducer with direct displacement measurement capability was designed and con-

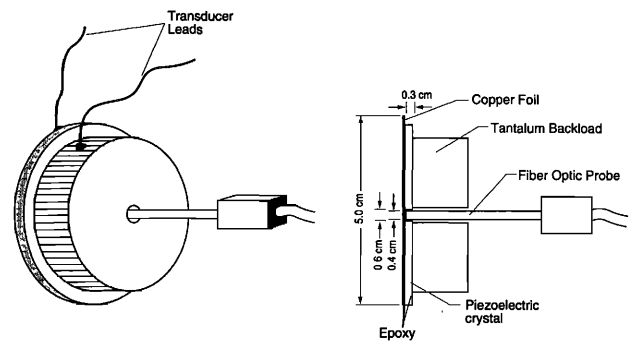


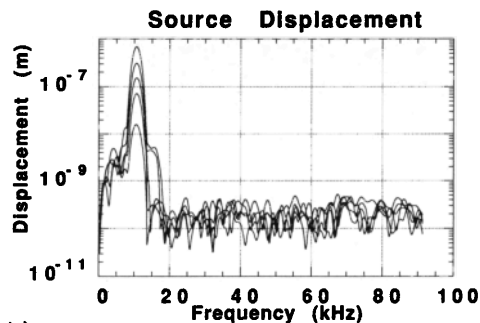
FIG. 2. Self-monitoring drive transducer for measurement of absolute displacement.

structed for use as the source. The source transducer consisted of a 5-cm-diam  $\times$  0.3-cm-thick piezoelectric crystal in which a 0.4-cm-diam hole was cut through its center, as shown in Fig. 2. A tantalum inertial backload was epoxied to the piezoelectric crystal and a thin piece of copper foil was epoxied to the face of the transducer for attachment of an electrical lead. The transducer was then epoxied to the end of the rod, as illustrated in Fig. 1. A Philtek ABH 88N2 fiber optic probe was positioned in the hole for a direct measurement of the displacement at the source. Assuming that the hole in the transducer is small in comparison to the wavelength of the acoustic signal, as was the case, the optical probe can be used to make measurements of the source displacement sensitive to  $10^{-9}$  m over a frequency range of dc to 200 kHz.

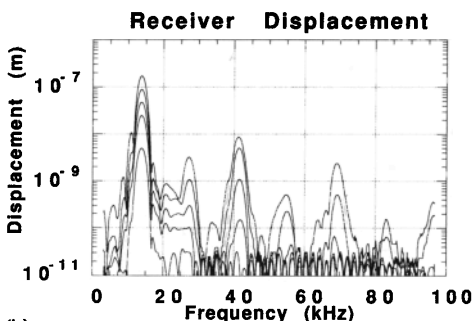
The source transducer was driven with a Hewlett-Packard 3314A function generator that was amplified by a Crown PSA-2 power amplifier. Typically, a single frequency or an amplitude modulated  $N$  cycle wave train of fixed length was input to the source transducer, where  $N$  ranged from 8–25. Frequencies of 8 to 24 kHz were used and care was taken to assure that there was no overlap with reflections from the opposite end of the rod in the measured signals. Detected signals were output to a 16-bit Analogic 6100B/652 waveform analyzer.

## III. RESULTS

The basic experimental observation providing evidence for the nonlinear behavior of the rock is shown in Fig. 3. In Fig. 3(a) we show the spectral composition of the displacement of the source transducer while being driven at 13.75 kHz. The five different curves correspond to five amplitudes of the source transducer varying over a factor of approximately 50. It is notable that, as the amplitude at the fundamental (drive) frequency was increased, the amplitude at frequencies other than the drive frequency remained very low (the  $2\omega$  harmonic is down by approximately two orders of magnitude from the fundamental and no higher harmonics are observed). In Fig. 3(b), we show the spectral composition for the five drive amplitudes after the signal has propagated 58 cm (about three wavelengths) from the source transducer. Comparison of Fig. 3(a) and (b) reveals the presence of rich harmonic content at 58 cm



(a)



(b)

FIG. 3. (a) Source spectra as measured with the optical probe for a 13.75-kHz drive. (b) Spectra after the wave has propagated 58 cm for a 13.75-kHz drive.

from the source transducer which does not exist at the source. Further, these higher harmonic displacement fields have amplitudes that are a sensitive function of the drive amplitude. We will return to a more careful look at the content of Fig. 3 below.

First, let us ask whether the nonlinear behavior we are seeing is the nonlinear behavior expected from the discussion in Sec. I. In what follows, we discuss the behavior of three important amplitudes. In order to avoid confusion, we list them here. They are: (1)  $u_1(x, 2\omega)$ , the amplitude of the signal at frequency  $2\omega$  and distance  $x$  from a source driven at frequency  $\omega$ ; (2)  $u_0(x, 2\omega)$ , the amplitude of the signal at distance  $x$  and frequency  $2\omega$  from a source driven at frequency  $2\omega$ ; and (3)  $u_0(x, \omega)$ , the amplitude of the signal at distance  $x$  and frequency  $\omega$  from a source driven at frequency  $\omega$ . In Sec. I we noted that there are three signatures of the  $2\omega$  harmonic generated by the nonlinearity in Eq. (1):

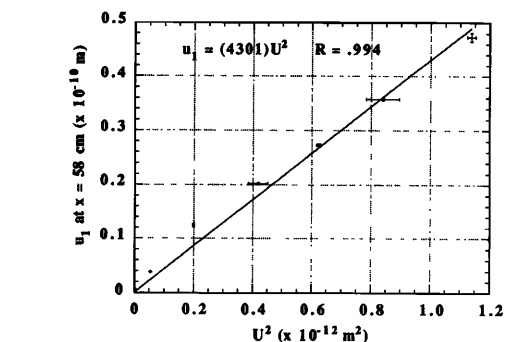


FIG. 5. Dependence of harmonic content on source amplitude,  $u_1(x, 2\omega) \propto U^2$  (14.6-kHz drive,  $x=58$  cm).

- (1)  $u_1(x, 2\omega) \propto x$ ,
- (2)  $u_1(x, 2\omega) \propto U^2$ ,
- (3)  $u_1(x, 2\omega) \propto \omega^2$ .

In Figs. 4–6, we show evidence that the observed  $2\omega$  harmonic has an amplitude that is consistent with these expectations.

In Fig. 4 we show the relative amplitude  $R$  of the first harmonic versus distance from the transducer for a 14.6-kHz drive. The relative amplitude is calculated by taking the ratio of the harmonic amplitude  $u_1(x, 2\omega)$  to the amplitude of a linear elastic wave of frequency  $2\omega$ ,  $u_0(x, 2\omega)$ . [The amplitude of the wave  $u_0(x, 2\omega)$  was relatively small, so it is assumed that it propagates linearly.] This ratio was taken in order to correct for transducer site effects and attenuation. According to Eq. (2), this ratio is proportional to the distance from the source:

$$R = \frac{u_1(x, 2\omega)}{u_0(x, 2\omega)} \propto x. \quad (3)$$

The result in Fig. 4 is in essential agreement with this prediction. [The fluctuations about the dashed line in Fig. 4 may be caused by position and frequency dependent elastic scattering from the periodic array of pinducers. As is explained in the Appendix, the effect of the periodic scatterers is to cause rapid spatial fluctuations in wave amplitude along the length of the rod and an effective increase in absorption in the rod. The measured attenuation in the rod

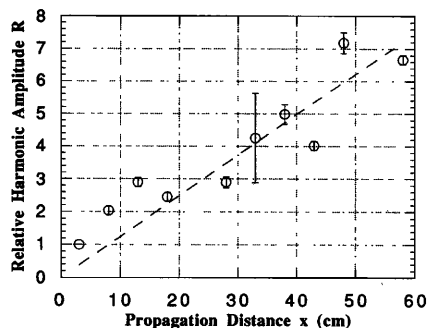


FIG. 4. Dependence of harmonic content on propagation distance,  $u_1(x, 2\omega) \propto x$  (14.6-kHz drive).

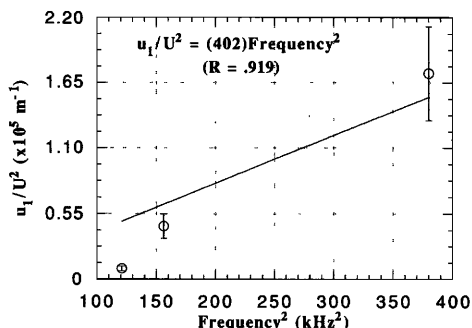


FIG. 6. Dependence of harmonic content on frequency,  $u_1(x, 2\omega)/U^2 \propto \omega^2$  ( $x=3$  cm).

implies that the quality factor  $Q$  is about 10, far lower than other measured values that range from 30–110 (Refs. 19 and 20). As the Appendix implies, the low  $Q$  measured here may be due to scattering.]

In Fig. 5 we show  $u_1(x, 2\omega)$  vs  $U^2$  at  $x=58$  cm for a drive frequency of 13.75 kHz. In order to form the ratio of  $u_1(x, 2\omega)$  to  $U^2$ , we calibrated the pinducers using the following procedure: (1) directly measure the displacement amplitude of the source using the optical probe described in Sec. II, and (2) determine the attenuation coefficient as a function of frequency (with low-input amplitude) by fitting the response of the pinducers as a function of  $x$  to

$$u_0(x, \omega) = Ue^{-\alpha(\omega)x}. \quad (4)$$

The absolute amplitude at  $x$ , found by combining (1) and (2), lets us calibrate the pinducers. This calibration had an uncertainty of about 25% due to the uncertainty in the measurement of  $\alpha$ . The error bars on the data indicate the scatter in the ratio over many measurements. The result shown in Fig. 5 strongly supports  $u_1(x, 2\omega) \propto U^2$ .

In Fig. 6 we show  $u_1(x, 2\omega)/U^2$  vs  $f^2 (= [\omega/2\pi]^2)$  measured at  $x=3$  cm. The quantity  $u_1(x, 2\omega)/U^2$  was measured as the best fit slope of  $u_1(x, 2\omega)$  vs  $U^2$  in plots like Fig. 5. The error bars were assigned according to the 25% measurement uncertainty determined from the calibration of the pinducers. The result shown in Fig. 6 strongly supports  $u_1(x, 2\omega) \propto \omega^2$ .

As a consequence of the agreement between the behavior of the observed  $2\omega$  harmonic amplitude and our model, Eq. (2), we feel confident that a significant portion of the observed response is due to the cubic anharmonicity of the elastic moduli of the rock. Thus we are justified in further analyzing the data using the model of Sec. I. From Eq. (2):

$$\frac{u_1(x, 2\omega)}{U^2 \omega^2} = \frac{\beta x}{2c^2},$$

where  $c = 2.60 \times 10^3 \pm 0.05 \times 10^3$  m/s,  $\omega/2\pi = 13.75 \pm 0.002$  kHz, and  $x = 3.0 \pm 0.5$  cm for the data in Fig. 6. Thus we calculate the compressional wave nonlinear parameter  $|\beta| = 7.0 \times 10^3 \pm 25\%$  for the sandstone sample assuming that attenuation is negligible. For the calculation of  $|\beta|$ , this is a reasonable assumption because the measured attenuation length ( $1/\alpha$ ) for 13.75 kHz is about 40 cm and the measurements used in the calculation were taken at  $x=3$  cm. This introduces a margin of error in  $|\beta|$ , which is within the measurement uncertainty of 25%. However, in general it may be necessary to incorporate attenuation into the theoretical description given by Eqs. (1) and (2). The inclusion of attenuation is considered by McCall.<sup>18</sup>

The results in Fig. 3(a) and (b) show spectral growth at the higher harmonics which are described by higher order terms in Eq. (1) and a higher order solution in Eq. (2). In particular, we find that the  $3\omega$  harmonic grows roughly proportional with  $U^3$ , a result which is in agreement with a second order correction to Eq. (2).<sup>18</sup> We also observe strong growth of the odd harmonics,  $3\omega$  and  $5\omega$ . This suggests that higher order terms (i.e., cubic anharmonic)

nicity) in the strain energy relationship may be necessary to give a complete description of nonlinear elasticity observations in rock.

#### IV. CONCLUSIONS

Large amplitude waves propagating in Berea sandstone were found to exhibit effects described by nonlinear elasticity theory. Measurements show an increase in the relative harmonic content with propagation distance and an increase in harmonic content with increasing source amplitude and frequency. From the frequency dependent measurements of harmonic content, a value for the compressional wave nonlinear parameter of Berea sandstone was calculated to be  $|\beta| = 7.0 \times 10^3 \pm 25\%$ . This result demonstrates the strong elastic nonlinearity that is characteristic of microcracked solids and that has also been observed in other disordered media.<sup>5,6,21</sup>

These results indicate that seismic wave propagation may include significant energy transfer between source frequencies and harmonics, and could ultimately affect the manner in which seismic sources are modeled. The agreement of our results with theory,<sup>18</sup> suggests that the theory could be successfully applied to seismic modeling.

In future work, we will study nonlinear effects in three dimensions and eventually over the seismic frequency band at varying temperature and pressure. We are also in the process of conducting laboratory experiments with a parametric array that we hope can eventually be used in the imaging of the Earth.

#### ACKNOWLEDGMENTS

This work was supported by the Office of Basic Energy Science of the U.S. Department of Energy under Contract No. W-7405-ENG-36 with Los Alamos National Laboratory. We thank Tom Shankland, Brian Bonner, Chris Angell, Igor Beresnev, Albert Migliori, and Tom Bell for their helpful contributions to the success of the experiments. We also thank Scott Phillips, Peter Roberts, Mike Fehler, Jim Rutledge, and Rick O'Connell for helpful discussions.

#### APPENDIX

The purpose of the discussion in this Appendix is to describe the influence of an (periodic) array of scatterers on the response of a one-dimensional elastic system. We include this discussion because the measured wave attenuation in the rod is orders of magnitude larger with the pinducers embedded in the rod than without the pins. We therefore accounted for the additional attenuation by use of the model described here. From McCall,<sup>18</sup> we see that in order to describe this response we require the Green's function for the linear response (i.e., both linear elasticity and linear attenuation) of the system. We use this Green function to propagate the disturbance at  $x=0$ , due to the external source, into the interior of the system. There, because of nonlinear elasticity, this disturbance serves as an internal source. Thus we also need the Green's function to propagate the disturbance from the internal source to the receiver transducers. When the interior of the sample con-

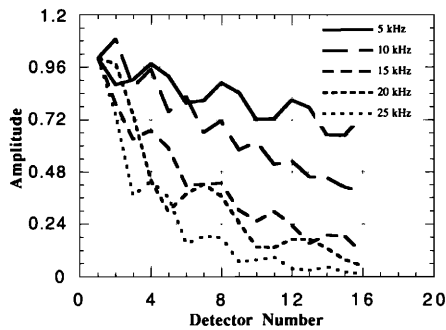


FIG. A1. Position and frequency-dependent scattering effects.

tains a sequence of scatterers, the Green's function called for must, in principle, be faithful to their presence. For the case at hand, the sequence of scatterers is the periodic array of transducers that are an integral part of the experimental system. So the Green's function needed is that for the propagation of a wave through a linear elastic material in the presence of a periodic sequence of scatterers. This Green's function can be developed (even for the case of a random array of scatterers) in terms of transfer matrices which carry the amplitudes of right-hand and left-hand going waves across the scattering regions. This is the so-called propagation matrix method used in a broad variety of problems. As our purpose here is to provide a qualitative explanation of important features seen in the data (the excess attenuation and the frequency-dependent amplitude fluctuations from one detector to the next), we will not write out the details of the solution to this problem. Rather, we will quote the results of several model calculations to illustrate these points and leave exhibition of the details to the future.

The computations required for the treatment of the problem at hand are essentially the same as those required to do the localization problem.<sup>22</sup> In Fig. A1 we show the amplitude at transducers 1–20 for elastic waves with frequencies of 5–25 kHz,  $Q=50$ , propagating into a material having the elastic properties of our sample. The 20 scatterers, spaced 5 cm from one another, are taken to be regions of width  $w$  having velocity of sound  $c_2 > c_1$ . While this model of the probes is not intended to be precise, it provides a simple realization of the important features in the structure of the transfer matrices that must characterize the probes. We note that in Fig. A1, while the intrinsic  $Q$  is of order 50, the apparent  $Q$  is of order 10. We also show the influence of frequency on the amplitude at detectors 1–20. Note that, as the frequency increases, so does the apparent attenuation due to scattering. At a fixed scattering sight, the amplitude, decaying on average more rapidly as frequency increases, fluctuates with frequency because of interference effects caused by the scatterers. These re-

sults are in qualitative and semiquantitative accord with experiment.

- <sup>1</sup> F. M. Pestorius and D. T. Blackstock, "Propagation of finite-amplitude noise," in *Finite-amplitude Wave Effects in Fluids, Proceedings of the 1973 Symposium—Copenhagen*, edited by L. Bjorno (Department of Fluid Mechanics, Technical University of Denmark, 1973), pp. 24–29.
- <sup>2</sup> M. F. Hamilton, "Fundamentals and applications of nonlinear acoustics," in *Nonlinear Wave Propagation in Mechanics—AMD-77* (The American Society of Mechanical Engineers, New York, 1986).
- <sup>3</sup> L. K. Zarembo and V. A. Krasil'nikov, "Some problems in the propagation of ultrasonic waves of finite amplitude in liquids," *Sov. Phys. Usp.* **2**(68), 580–599 (1959).
- <sup>4</sup> A. A. Gedroits and V. A. Krasil'nikov, "Finite-amplitude waves in solids and deviations from Hooke's law," *Sov. Phys. JETP* **16**, 1122–1126 (1963).
- <sup>5</sup> L. A. Ostrovsky, "Wave processes in media with strong acoustic nonlinearity," *J. Acoust. Soc. Am.* **90**, 3332–3337 (1991).
- <sup>6</sup> V. N. Bakulin and A. G. Protosenya, "Nonlinear effects in travel of elastic waves through rocks," *Trans. (Dokl.) USSR Acad. Sci. Earth Sciences Sec.* **263**, 314–316 (1981).
- <sup>7</sup> P. A. Johnson, T. J. Shankland, R. J. O'Connell, and J. N. Albright, "Nonlinear generation of elastic waves in crystalline rock," *J. Geophys. Res.* **92**, 3597–3602 (1987).
- <sup>8</sup> P. A. Johnson and T. J. Shankland, "Nonlinear generation of elastic waves in granite and sandstone: Continuous wave and travel time observations," *J. Geophys. Res.* **94**, 17,729–17,733 (1989).
- <sup>9</sup> I. A. Beresnev and A. V. Nikolaev, "Experimental investigations of nonlinear seismic effects," *Phys. Earth Planetary Int.* **50**, 83–87 (1988).
- <sup>10</sup> P. A. Johnson, T. M. Hopson, and T. J. Shankland, "Frequency domain travel time (FDTT) measurement of ultrasonic waves by use of linear and nonlinear sources," *J. Acoust. Soc. Am.* **92**, 2842–2850 (1992).
- <sup>11</sup> G. P. Zinov'yeva, I. I. Nesterov, Y. L. Zhdakhin, E. E. Artma, and Y. V. Gorbunov, "Investigation of rock deformation properties in terms of the nonlinear acoustic parameter," *Trans. (Dokl.) USSR Acad. Sci. Earth Science Sec.* **307**, 337–341 (1989).
- <sup>12</sup> B. P. Bonner and B. J. Wanamaker, "Acoustic nonlinearities produced by a single macroscopic fracture in granite," in *Review of Progress in Quantitative NDE*, edited by D. O. Thompson and D. E. Chimenti (Plenum, New York, 1991), Vol. 10B, pp. 1861–1867.
- <sup>13</sup> L. D. Landau and E. M. Lifshitz, *Theory of Elasticity, 3rd Edition* (Pergamon, Oxford, 1986), pp. 9–11.
- <sup>14</sup> F. D. Murnaghan, *Finite Deformation of an Elastic Solid* (Wiley, New York, 1951).
- <sup>15</sup> R. E. Green, Jr., *Treatise on Materials Science and Technology, Vol. 3, Ultrasonic Investigation of Mechanical Properties* (Academic, New York, 1973), pp. 76–78.
- <sup>16</sup> Z. A. Gol'dberg, "Interaction of plane longitudinal and transverse elastic waves," *Sov. Phys.-Acoust.* **6**, 307–310 (1959).
- <sup>17</sup> A. L. Polyakova, "Nonlinear effects in a solid," *Sov. Phys.-Solid State* **6**, 50–54 (1964).
- <sup>18</sup> K. R. McCall, "Theoretical study of nonlinear elastic wave propagation," *J. Geophys. Res.* (in press).
- <sup>19</sup> A. L. Frisillo and T. J. Stewart, "Effect of partial gas/brine saturation on ultrasonic absorption in sandstone," *J. Geophys. Res.* **85**, 5209–5211 (1980).
- <sup>20</sup> K. W. Winkler and A. Nur, "Seismic attenuation: Effects of pore fluids and frictional sliding," *Geophysics* **47**, 1–14 (1982).
- <sup>21</sup> I. Yu. Belyaeva, A. M. Sutin, and V. Yu. Zaitsev, "Tomography of the acoustical parameter: possible applications to seismics," in *Advances in Nonlinear Acoustics, Proceedings of the 13th International Symposium on Nonlinear Acoustics*, edited by H. Hobaek (World Scientific, Singapore, 1993), pp. 376–381.
- <sup>22</sup> D. T. Smith, C. P. Lorenson, R. B. Hallock, K. R. McCall, and R. A. Guyer, "Third sound on substrates patterned with periodic and random disorder: Evidence for classical wave localization," *Phys. Rev. Lett.* **61**, 1286 (1988).